



**Oxidovanadium(IV), Oxidomolybdenum(VI) and Cobalt(III)
Complexes of o-Phenylenediamine Derivatives: Oxidative
Dehydrogenation and Photoluminescence**

Journal:	<i>Inorganic Chemistry Frontiers</i>
Manuscript ID:	QI-ART-12-2013-000103.R1
Article Type:	Paper
Date Submitted by the Author:	20-Jan-2014
Complete List of Authors:	Ghosh, Prasanta; R. K. Mission Residential College, Dept of Chemistry Chaudhuri, Satyabrata; R. K. M. Residential College, Narendrapur, Department of Chemistry Bera, Sachinath; R. K. M. Residential College, Narendrapur, Department of Chemistry Biswas, Manas; RKM Residential College, Department of Chemistry Saha Roy, Amit; R. K. M. Residential College, Narendrapur, Department of Chemistry Weyhermueller, Thomas; Max-Planck-Institut für Chemische Energiekonversion,

ARTICLE

Oxidovanadium(IV), Oxidomolybdenum(VI) and Cobalt(III) Complexes of *o*-Phenylenediamine Derivatives: Oxidative Dehydrogenation and Photoluminescence[†]

Cite this: DOI: 10.1039/x0xx00000x

Received 00th January 2012,
Accepted 00th January 2012

DOI: 10.1039/x0xx00000x

www.rsc.org/

Satyabrata Chaudhuri,^a Sachinath Bera,^a Manas Kumar Biswas,^a Amit Saha Roy,^a Thomas Weyhermüller^b and Prasanta Ghosh^{*,a}

Reactions of *o*-phenylenediamine derivatives (L₃H₂) incorporating a (Ph)(Py)(H)C-N(H)-function with the oxidovanadium(IV) and oxidomolybdenum(VI) ions afford amide complexes of types [V^{IV}O(L₃²⁻)] (3), [V^{IV}O(L₃^{t-Bu 2-})] (4) and *cis*-[Mo^{VI}O₂(L₃²⁻)] (5) (L₃H₂ = (*E*)-2-(((2-((phenyl(pyridin-2-yl)methyl)amino)phenyl)imino)methyl)phenol); L₃^{t-BuH} = (*E*)-2,4-di-tert-butyl-6-(((2-((phenyl(pyridin-2-yl)methyl)amino)phenyl)imino)methyl)phenol), while the similar reaction of L₃H₂ with the anhydrous CoCl₂ in air results oxidative dehydrogenation (OD) of the (Ph)(Py)(H)C-N(H)-function affording a cobalt(III) diimine complex, *trans*-[Co^{III}(L₄⁻)Cl₂] (6) (L₄H = 2-((*E*)-(2-((*E*)-phenyl(pyridin-2-yl)methyleneamino)phenylimino)methyl)phenol) contradicting the participation of the higher oxidation states of the metal ions in OD reaction of amines. 3-6 are characterized by the elemental analyses, mass, IR, ¹H NMR and EPR spectra. The molecular geometries of 4.CH₃OH, 5 and 6 were confirmed by the single crystal X-ray structure determinations. The V^{IV}-O_{phenolato} cis to the V=O bond and the V^{IV}=O lengths in 4.CH₃OH are 1.925(2) and 1.612(2) Å. Two cis Mo=O lengths are 1.710(2) Å and 1.720(2) Å in 5. The aliphatic -C-N- lengths, in 4.CH₃OH and 5 are 1.448(3) and 1.479(2) Å, while the same is 1.285(4) Å in 6. DFT calculations on 3 and 6 inferred a significant mixing among d_M and NN-ligand backbone favoring a t₂⁶ state of the metal ion for the OD of the amine fragment to have stronger d_M → π_{ketimine}^{*} back-bonding. The π_{NHPh} → π_{aldimine}^{*} transition of L₃H₂ is red shifted in 3 and 4 quenching the emissive π_{phenolato} → π_{aldimine}^{*} transitions, elucidated by the TD DFT calculations on 3 (and 3⁺). The π_{NPh} → π_{aldimine}^{*} transitions are blue shifted in the oxidovanadium(V) analogues, [V^VO(L₃²⁻)]⁺ (3⁺) and [V^VO(L₃^{t-Bu 2-})]⁺ (4⁺) which are fluorescent (3⁺, λ_{ex} = 331, λ_{em} = 444 nm; 4⁺, λ_{ex} = 339, λ_{em} = 490 nm) recorded by the fluorescence-spectroelectrochemical measurements in CH₂Cl₂. 5 and 6 emit weakly at 466 and 473 nm (5, λ_{ex} = 336 nm, φ = 0.003; 6, λ_{ex} = 324 nm, φ = 0.027).

Introduction

Oxidation of amine is a significant reaction in biology.¹ In laboratory, transition metal promoted oxidative dehydrogenation (OD) reaction of amine has been an area of research since 1960 and the reaction was first reported by Curtis *et al.*² Till date, several OD reactions mediated by the transition metal ions with different mechanistic aspects were reported.³ In many cases participation of the transition metal ions to the -(2e+2H⁺) transfer reaction has been proposed. The accepted mechanism is that the metal ion is oxidized first to a higher oxidation state that will either stepwise oxidize amine by 1e⁻ transfer *via* a ligand radical intermediate or directly by 2e⁻ transfer eliminating protons.³ It was reported that the OD

reactions of [Ru(bpy)₂(ampy)]²⁺ (ampy = 2-(aminomethyl)pyridine)^{4a}, [Ru(tame)₂]²⁺ (tame = 1,1,1-tris(aminomethyl)ethane)^{4b}, [Ru(en)₃]³⁺ (en = ethylenediamine)^{4b} [Ru(sar)]²⁺ (sar = sarcophagine, 3,6,10,13,16,19-hexaazabicyclo(6,6,6)eicosane)^{4c}, and [Ru(bpy)₂(NC₅H₄CH(CH₃)OH)]²⁺ (NC₅H₄CH(CH₃)OH) = 2-(hydroxymethyl)pyridine)^{4d} undergo *via* ruthenium(IV) intermediate. Similarly, intermediacy of M(IV) ion was proposed in the OD reactions of [Os(bpy)₂(ampy)]²⁺^{4e}, [Os(en)₃]³⁺^{4f} and [Fe(sar)]³⁺^{3a} complexes. A Ni(III) intermediate also was proposed to participate in the OD reaction of tetraazamacrocyclic complex of nickel(II) ion.^{4g} However, the proposals of the participation of Fe(IV), Ni(III), Os(IV), Ru(IV) ions in OD reactions are futile.

The reduction of the metal ion during OD reactions has been established only in cases of copper(II), iron(III) and ruthenium(III) ions isolating their reduced analogues. Reduction of copper(II) to copper(I) has been established in OD reactions of $[\text{Cu}^{\text{II}}(\text{H}_4\text{L})]^{4+}$ (L = octaazamacrocyclic dinucleating ligand)^{5a}, Cu^{II} (boradiazaindacene (BODIPY) derivative)^{5b} and $[\text{Cu}^{\text{II}}(\text{L})]^{2+}$ (L = *N,N*-bis-quinolin-2-ylmethyl-cyclohexane-*trans*-1,2-diamine)^{5c} complexes. Reduction of iron(III) to iron(II) in the OD reactions of $[\text{Fe}^{\text{III}}\text{H}_2\text{L}]^{3+}$ (H_2L = 1,9-bis(2'-pyridyl)-5-[(ethoxy-2''-pyridyl)methyl]-2,5,8-triazanonane)^{5d}, teracyano(1,2-diamine derivative)ferrate(III)^{5e} complexes and formation of ruthenium(II) analogue in the OD reaction of $[\text{Ru}^{\text{III}}(\text{O-N})(\text{bpy})_2]^{2+}$ (O-N = unsymmetrical bidentate phenolate type ligand, bpy = 2,2'-bipyridine)^{5f} were authenticated. However, the reports of air and base promoted OD reactions of the amine complexes of nickel(II), cobalt(III) and rare earth metal ions are significant.^{5g-i}

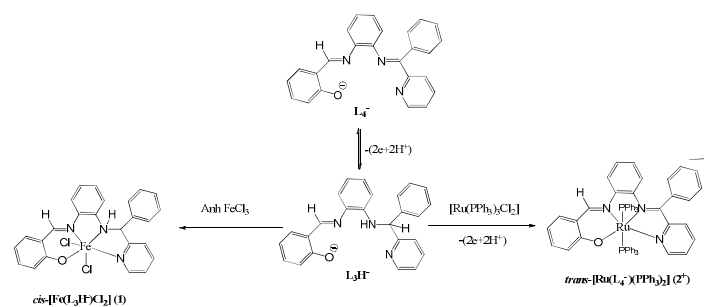
o-Phenylene diamine derivatives are strong chelating agents and furnished several bioactive transition metal complexes.⁶ Thus, the coordination chemistry of *o*-phenylenediamine derivatives is a subject of investigation here. Recently, we reported the OD reaction of a tetradentate *o*-phenylenediamine derivative (L_3H_2) (L_3H_2 = (*E*)-2-(((2-((phenyl(pyridin-2-yl)methyl)amino)phenyl)))). It was disclosed that the reaction of L_3H_2 with tris(triphenylphosphine)ruthenium(II) precursor results the OD reaction converting L_3H^+ to L_4^- affording *trans*- $[\text{Ru}(\text{L}_4^-)(\text{PPh}_3)_2]^+$ (2^+) cation (L_4H = 2-((*E*)-2-((*E*)-phenyl(pyridinyl)methyleneamino)phenylimino)methyl)phenol.⁷ However, in presence of an easily reducible iron(III) ion, no OD reaction occurs and the reaction ends up with the formation of an amine complex, *cis*- $[\text{Fe}(\text{L}_3\text{H})\text{Cl}_2]$ (**1**), as shown in Scheme 1.

In this work the role of the metal ions in the OD reaction of the (Ph)(Py)(H)C-N(H)- function of L_3H_2 was further investigated. The question is whether the reaction requires the higher oxidation states of the metal ions to promote the OD reaction acclaimed so far. To explore it, the chemistry of L_3H_2 towards the oxidovanadium(IV) and oxidomolybdenum(VI) ions which are redox active and participate in electron transfer reaction at lower potential and at neutral pH in several redoxenzymes has been investigated.^{8,9} Further, oxidovanadium(IV) and dioxidomolybdenum(VI) complexes were reported as effective catalysts for oxo transfer^{10a}, epoxidation of olefins^{10b}, hydrosilylation of carbonyls^{10c} and oxidative bromination^{10d} reactions. The reactions of oxidovanadium(IV), oxidomolybdenum(VI) and cobaltous ions with L_3H_2 and $\text{L}_3^{\text{t-Bu}}\text{H}_2$ in air were performed. Surprisingly, the OD reaction does not occur with oxidizing oxidovanadium(IV) and oxidomolybdenum(VI) ions yielding only the amide products, as $[\text{V}^{\text{IV}}\text{O}(\text{L}_3^{2-})]$ (**3**), $[\text{V}^{\text{IV}}\text{O}(\text{L}_3^{\text{t-Bu}2-})]$ (**4**) and *cis*- $[\text{Mo}^{\text{VI}}\text{O}_2(\text{L}_3^{2-})]$ (**5**) ($\text{L}_3^{\text{t-Bu}}\text{H}_2$ = (*E*)-2,4-di-tert-butyl-6-(((2-((phenyl(pyridin-2-yl)methyl)amino)phenyl)imino)methyl)phenol), while the cobaltous ion promotes the OD reaction affording a cobalt(III) complex of the ketimine derivative, *trans*- $[\text{Co}^{\text{III}}(\text{L}_4^-)\text{Cl}_2]$ (**6**).

The metal ion dependent fluorescence features of the organic chromophore is a significant investigation.¹¹ It is observed that L_3H_2 is fluorescent due to the internal charge transfer (ICT) from the $\pi_{\text{phenolato}}$ to the π_{aldimine^*} orbital ($\lambda_{\text{ex}} = 330$; $\lambda_{\text{em}} = 470$ nm)⁷. Lifetimes measurements and time resolved emission spectra (TRES) have confirmed that the lower energy excited state at 390 nm has a higher non-radiative rate constant (k_{nr}). It was noted that due to the molecular aggregation at higher concentration, the fluid solution fluorescence spectra of L_3H_2 depend on concentration, which has been investigated by ¹H NMR and temperature dependent fluorescence spectra.⁷ The interesting observation is that the molecular aggregation of L_3H_2 depends reversibly on temperature. At higher concentration, in addition to the emission band at 470 nm, L_3H_2 displays a lower energy emission band at 525 nm which disappears upon dilution. It was recorded that **1** is eighty fold stronger emissive than L_3H_2 itself, while the ketimine analogue 2^+ ion is non-emissive.⁷ The fluid solution fluorescence features of **3**, **4**, **5** and **6** are also recorded at 298 K. It is found that **3** and **4** in fluid solutions at 298 K are non emissive while the electrogenerated one-electron oxidized analogues, $[\text{V}^{\text{VO}}(\text{L}_3^{2-})]^+$ (3^+) and $[\text{V}^{\text{VO}}(\text{L}_3^{\text{t-Bu}2-})]^+$ (4^+) are emissive. The complex **5** is weakly emissive. The fluorescence of L_3H_2 ligand is completely quenched in presence of reducing cobalt(II) ion, while **6** is brightly emissive.

In this article to substantiate the role of the metal ions in the OD reaction of the of L_3H_2 , syntheses, spectra and X-ray structures including the diverse fluorescence spectra and the redox series of **3**, **4**, **5** and **6** are reported. Density functional theory (DFT) and the time dependent (TD) DFT calculations were performed to elucidate the fluorescent as well as the quenched electronic states of the complexes.

Scheme 1



Experimental section

Materials and physical measurements

Reagents or analytical grade materials were obtained from the commercial suppliers and used without further purification. $\text{VO}(\text{acac})_2$ (acac = acetylacetonate) was prepared by the reported procedure.^{10e} Spectroscopic grade solvents were used for spectroscopic and electrochemical measurements. After evaporating MeOH solvents of the sample under high vacuum, elemental analyses and spectral measurements were performed. The C, H and N content of the compounds were obtained from

Perkin-Elmer 2400 series II elemental analyzer. Infrared spectra of the samples were measured from 4000 to 400 cm^{-1} with the KBr pellet at room temperature on a *Perkin-Elmer Spectrum RX 1* FT-IR Spectrophotometer. ^1H NMR spectra in CDCl_3 were carried out on a *Bruker DPX-300 MHz* spectrometer with tetramethylsilane (TMS) as an internal reference. ESI mass spectrum was recorded on a *micromass Q-TOF* mass spectrometer. Electronic absorption spectra in solutions at 298 K were recorded on a *Perkin-Elmer Lambda 750* spectrophotometer in the range of 3000-200 nm. Magnetic susceptibility at 298 K was measured on Sherwood Magnetic Susceptibility Balance. The electro analytical instrument, *BASi Epsilon-EC* for cyclic voltammetric experiment in CH_2Cl_2 solutions containing 0.2 M tetrabutylammoniumhexafluoro phosphate as supporting electrolyte was used. The BASi platinum working electrode, platinum auxiliary electrode, Ag/AgCl reference electrode were used for the measurements. The redox potential data are referenced vs. ferrocenium / ferrocene, Fc^+ / Fc , couple. In all cases, the experiments were performed with the multiple scan rates to analyze the reversibility of the electron transfer waves. BASi Epsilon-EC has been used for spectroelectrochemistry measurements. The X-band electron paramagnetic resonance (EPR) spectra were measured on a Magnostech GmbH MiniScope MS400 spectrometer (equipped with temperature controller TC H03), where the microwave frequency was measured with a frequency counter FC400.

The EPR spectra of the CH_2Cl_2 solutions of the paramagnetic **3** and **4** were recorded at 298 K. The EPR spectrum of the CH_2Cl_2 frozen glass of **3** at 25 K was also recorded. The fluorescence spectra of the complexes were recorded in CH_2Cl_2 at 298 K. The spectral features of 3^+ and 4^+ ions were recorded by fluorescence spectro-electrochemical measurements in CH_2Cl_2 solvent at 298 K.

Excitation and emission spectra were recorded using quartz sample tube on *Perkin Elmer LS 55* luminescence spectrophotometer. Fluorescence quantum yield (ϕ_D) was determined in each case by comparing the corrected emission spectrum of the samples with that of the anthracene in MeOH ($\phi_D = 0.20$) and CH_2Cl_2 ($\phi_D = 0.30$) using the equation¹² considering the total area under the emission curve.

$$Q = Q_R \frac{F}{F_R} \frac{OD_R n^2}{OD n_R^2} \quad (1)$$

where Q is the quantum yield of the compounds, F is the integrated fluorescence intensity (area under the emission curve), OD is the optical density, and n is the refractive index of the medium. It is assumed that the reference and the unknown samples are excited at the same wavelength. The subscript R refers to the reference fluorophore (anthracene in this case) of known quantum yield. The standard quantum yield value thus obtained is used for the calculation of quantum yields of the systems under various conditions.

Syntheses

(E)-2-((2-(phenyl(pyridin-2-yl)methylamino)phenyl imino)methyl)phenol (L_3H_2). It was prepared by a reported

procedure from a zinc complex, $[\text{Zn}(\text{L}_1)\text{Cl}_2]$ ($\text{L}_1 = (E)\text{-N}^1\text{-(phenyl(pyridin-2-yl)methylene)benzene-1, 2-diamine}$).⁷

(E)-2,4-di-tert-butyl-6-((2((phenyl(pyridin2yl)methyl amino)phenyl)imino)methyl)phenol ($\text{L}_3^{\text{t-Bu}}\text{H}_2$). It was prepared using $[\text{Zn}(\text{L}_1)\text{Cl}_2]$ as a precursor. To a MeOH solution (25 ml) of $[\text{Zn}(\text{L}_1)\text{Cl}_2]$ (410 mg, 1 mmol), sodiumborohydride was added by parts with constant stirring until the reddish orange solution turned light yellow. The solution was evaporated under low pressure and the residue was extracted with diethyl ether. After evaporation the ether solution, a yellow oily liquid of L_2H was obtained ($\text{L}_2\text{H} = \text{N}^1\text{-(Phenyl(pyridin-2-yl)methyl)benzene-1, 2-diamine}$).⁷ To L_2H , MeOH (10 ml) followed by 3, 5-ditertbutyl-2-hydroxy benzaldehyde (240 mg, 1 mmol) were added and the resulting solution was heated to reflux for 30 min and cooled at 298 K. A yellow crystalline solid of $\text{L}_3^{\text{t-Bu}}\text{H}_2$ separated out which was filtered and dried in air. Yield: 110 mg (60% with respect to 2-benzoyl pyridine). Mass spectral data (ESI, positive ion, CH_3OH): m/z 492 for $[\text{L}_3^{\text{t-Bu}}\text{H}_2]^+$. ^1H NMR (CDCl_3 , 300 MHz): δ (ppm) 13.54 (s, 1H), 8.65 (s, 1H), 8.60 (d, 1H), 7.59 (t, 1H), 7.52 (t, 3H), 7.32 (m, 3H), 7.07 (m, 3H), 6.69 (t, 3H), 6.54 (t, 2H) 5.61 (d, 1H), 1.51 (s, 9H), 1.35 (s, 9H). Anal. Calcd (%) for $\text{C}_{33}\text{H}_{37}\text{N}_3\text{O}$: C, 80.61; H, 7.59; N, 8.55. Found: C, 80.10; H, 7.37; N, 8.42. IR / cm^{-1} (KBr): ν 3370 (vs), 2962 (vs), 1595 (vs), 1508 (vs), 1437 (s), 1330 (s), 1250 (s), 998 (s), 754 (s), 581 (m).

$[\text{V}^{\text{IV}}\text{O}(\text{L}_3^2)]$ (3**).** To a MeOH solution (30 ml) of L_3H_2 (380 mg, 1 mmol), $\text{VO}(\text{acac})_2$ (260 mg, 1 mmol) was added and the resulting solution was heated at 327 K for 10-15 min. The solution was cooled at 298 K and filtered. The filtrate was allowed to evaporate slowly in air. After 2-3 days, a dark brown crystalline compound of **3** separated out, which was filtered and dried in air. Yield: 20 mg (40% with respect to vanadium). Mass spectral data (ESI, positive ion, CH_3OH): m/z 445 for $[\mathbf{3}]^+$. Anal. Calcd (%) for $\text{C}_{25}\text{H}_{19}\text{N}_3\text{O}_2\text{V}$: C, 67.57; H, 4.31; N, 9.46. Found: C, 65.98; H, 4.15; N, 9.41. IR / cm^{-1} (KBr): ν 3411 (m), 3055 (m), 1604 (vs), 1528 (s), 1464 (vs), 1381 (vs), 1328 (vs), 1202 (m), 1154 (s), 1030 (m), 960 (vs), 844 (m), 739 (vs), 707 (s), 555 (s), 409 (m).

$[\text{V}^{\text{IV}}\text{O}(\text{L}_3^{\text{t-Bu} 2-})]\cdot\text{CH}_3\text{OH}$ (4.CH₃OH**).** To a MeOH solution (30 ml) of $\text{L}_3^{\text{t-Bu}}\text{H}_2$ (492 mg, 1 mmol), $\text{VO}(\text{acac})_2$ (260 mg, 1 mmol) was added and the resulting solution was heated at 327 K for 10-15 min. The solution was cooled at 298 K and filtered. The filtrate was allowed to evaporate slowly in air. After 2-3 days, a dark brown crystalline compound of **4.CH₃OH** separated out, which was filtered and dried in air. Yield: 23 mg (45% with respect to vanadium). Mass spectral data (ESI, positive ion, CH_3OH): m/z 557 for $[\mathbf{4}]^+$. Anal. Calcd (%) for $\text{C}_{33}\text{H}_{35}\text{N}_3\text{O}_2\text{V}$: C, 71.21; H, 6.34; N, 7.55. Found: C, 70.18. H, 6.19; N, 7.41. IR / cm^{-1} (KBr): ν 3422 (m), 2949 (s), 1597 (vs), 1477 (vs), 1382 (s), 1326 (vs), 1169 (s), 1031 (m), 954 (vs), 760 (s), 734 (vs), 702 (m), 570 (m).

***cis*- $[\text{Mo}^{\text{VI}}\text{O}_2(\text{L}_3^2)]$ (**5**).** To a MeOH solution (30 ml) of L_3H_2 (380 mg, 1 mmol), $(\text{NH}_4)_2[\text{MoO}_4]$ (175 mg, 1 mmol) was

added and the resulting solution was heated at 327 K for 60 min. The orange-yellow solid of **5** separated out, which was filtered, dried in air and collected. The product was further recrystallized by diffusing *n*-hexane to the CH₂Cl₂ solution of the crude product at 298 K for single crystal X-ray structure determination. Yield: 120 mg (~68% with respect to molybdenum). Mass spectral data (ESI, positive ion, CH₃OH): *m/z* 507.89 for [**5**]. ¹H NMR (CDCl₃, 300 MHz): δ(ppm) 8.66 (s, 1H), 8.34(d, 1H), 7.79(t, 1H), 7.61-7.43 (m, 5H), 7.37-7.35 (m, 5H), 7.18-6.91 (m, 4H), 6.37 (s, 1H), 5.30 (s, 1H). Anal. Calcd (%) for C₂₅H₁₉MoN₃O₃: C, 59.41; H, 3.79; N, 8.31. Found: C, 58.75; H, 3.62; N, 8.15. IR / cm⁻¹ (KBr): ν 1614 (vs), 1600 (s), 1547 (s), 1472 (s), 1441 (m), 1384 (m), 1233 (m), 1022 (s), 901 (vs), 915 (vs), 886 (vs), 796 (m), 746 (s), 694 (m), 624 (m).

trans-[Co^{III}(L₄)Cl₂] (6). To a MeOH solution (30 ml) of L₃H₂ (380 mg, 1 mmol), anhydrous CoCl₂ (136 mg, 1 mmol) was added and the resulting solution was heated at 327 K for 60 min. The solution was cooled at 298 K and filtered. The filtrate was allowed to evaporate slowly in air. After 2-3 days, a dark brown crystalline compound of **6** separated out, which was filtered and dried in air. Yield: 90 mg (~66% with respect to cobalt). Mass spectral data (ESI, positive ion, CH₃OH): *m/z* 435 for [**6**-2Cl]⁺. ¹H NMR (CDCl₃, 300 MHz): δ(ppm) 10.04 (s, 1H), 8.73 (s, 1H), 8.53 (s, 3H), 7.79 (m, 3H), 7.89-6.16 (m, 10H). Anal. Calcd (%) for C₂₅H₁₈Cl₂CoN₃O: C, 59.31; H, 3.58; N, 8.30. Found: C, 58.95; H, 3.52; N, 8.15. IR / cm⁻¹ (KBr): ν 3422 (s), 1609 (vs), 1528 (s), 1438 (m), 1384 (m), 1350 (m), 1145 (m), 754 (m).

X-Ray crystallographic data collection and refinement of the structures (CCDC 842402(**6**), 972492(**4.CH₃OH**) and 972493 (**5**))

Single crystals of **4.CH₃OH**, **5** and **6** were picked up with nylon loops and were mounted on a 'Bruker AXS Enraf-Nonius Kappa CCD' diffractometer equipped with a Mo-target rotating-anode X-ray source and a graphite monochromator (Mo-Kα, λ = 0.71073 Å). **4.CH₃OH** and **5** were measured at 100 K while **6** was measured at 296 K. Final cell constants were obtained from least squares fits of all measured reflections. The intensity data was corrected for absorptions using intensities of redundant reflections. The structures were readily solved by direct methods and subsequent different Fourier techniques. The crystallographic data of **4.CH₃OH**, **5** and **6** are listed in Table 1.

The Siemens *SHELXS-97*^{13a} and *SHELXL-97*^{13b} software packages were used for solution and the refinement. All non-hydrogen atoms were refined anisotropically. Hydrogen atoms were placed at the calculated positions and refined as riding atoms with isotropic displacement parameters.

Density functional theory (DFT) calculations

All the calculations reported in this article were done with the *Gaussian 03W*¹⁴ program package supported by *GaussView 4.1*. The DFT¹⁵ and TD DFT¹⁶ calculations were performed at the

Table 1 X-ray crystallographic data for **4.CH₃OH**, **5** and **6**

	4.CH₃OH	5	6
formula	C ₃₃ H ₃₅ N ₃ O ₂	C ₂₅ H ₁₉ MoN ₃ O ₃	C ₂₅ H ₁₈ Cl ₂ CoN ₃ O
fw	572.60	505.37	506.21
cryst color	red	orange	green
cryst syst	Triclinic	Triclinic	Monoclinic
space group	<i>P</i> -1	<i>P</i> -1	<i>P</i> 2 ₁ / <i>c</i>
<i>a</i> (Å)	9.340(3)	7.9292(2)	9.3416(5)
<i>b</i> (Å)	11.616(7)	11.4808(6)	12.8676(7)
<i>c</i> (Å)	13.836(4)	11.7269(9)	19.8225(11)
<i>a</i> (deg)	76.22(5)	76.524(4)	90.00
<i>β</i> (deg)	83.19(5)	83.276(5)	103.333(3)
<i>γ</i> (deg)	88.86(5)	81.837(3)	90.00
<i>V</i> (Å ³)	1447.6(11)	1023.71(10)	2318.5(2)
<i>Z</i>	2	2	4
<i>T</i> (K)	100(2)	100(2)	296(2)
<i>2θ</i>	60.00	62.00	48
calcd (g cm ⁻³)	1.314	1.640	1.450
reflns collected	18275	15702	9921
unique reflns	8372	6499	3489
reflection [<i>I</i> > 2σ(<i>I</i>)]	5603	6061	2567
λ (Å) / μ (mm ⁻¹)	0.71073/0.380	0.71073/0.675	0.71073/0.993
F(000)	604	512	1032
R1 ^a [<i>I</i> > 2σ(<i>I</i>)] / GOF ^b	0.0682/1.036	0.0263/1.059	0.0432/1.051
R1 ^a (all data)	0.1118	0.0293	0.0609
wR2 ^c [<i>I</i> > 2σ(<i>I</i>)]	0.1469	0.0675	0.1145
no. of param. / restr.	378/0	289/0	289/0
residual density (eÅ ⁻³)	0.852	0.729	0.432

^aR1 = Σ||F_o - F_c|| / ΣF_o, ^bGOF = {Σ[w(F_o² - F_c²)²] / (n-p)}^{1/2}; ^cwR2 = [Σ[w(F_o² - F_c²)²] / Σ[w(F_o²)²]]^{1/2} where w = 1/[σ²(F_o²) + (aP)² + bP], P = (F_o² + 2F_c²) / 3.

level of the Becke three parameter hybrid functional with the non-local correlation functional of Lee–Yang–Parr (B3LYP).¹⁷ The gas-phase geometries of **3** with doublet spin state, **3⁺** and **6** with singlet spin state were optimized using Pulay's Direct Inversion¹⁸ in the iterative Subspace (DIIS), 'tight' convergent SCF procedure¹⁹ ignoring symmetry. The optimized coordinates are listed in Tables S8–S11 (SI[†]). In all the calculations, a LANL2DZ basis set²⁰, along with the corresponding effective core potential (ECP) was used for the metal atom. Valence double Zeta with polarization and diffuse functional basis set, 6-31++G**²¹ were used for the C, N, O and Cl atoms in all the calculations. For the H atoms, the 6-31G basis set was used.²² The percentage contributions of the metal, chloride and ligand to the frontier orbital of the optimized geometries were calculated using the GaussSum program package.²³ The sixty excitation energies on the optimized geometries of **3**, **3⁺** and **6** were calculated by TD DFT²⁴ calculations.

Results and discussion

The coordination complexes of the amide and imine derivatives of L₃H₂ isolated in this work are depicted in Scheme 2. Details of the syntheses of **3–6** are given in the experimental section. *o*-Phenylene derivatives are synthesized by the reported procedures⁷. L₃^{t-Bu}H₂ and **3–6** are characterized by the elemental analyses, IR, mass, EPR and ¹H NMR spectra. The V=O

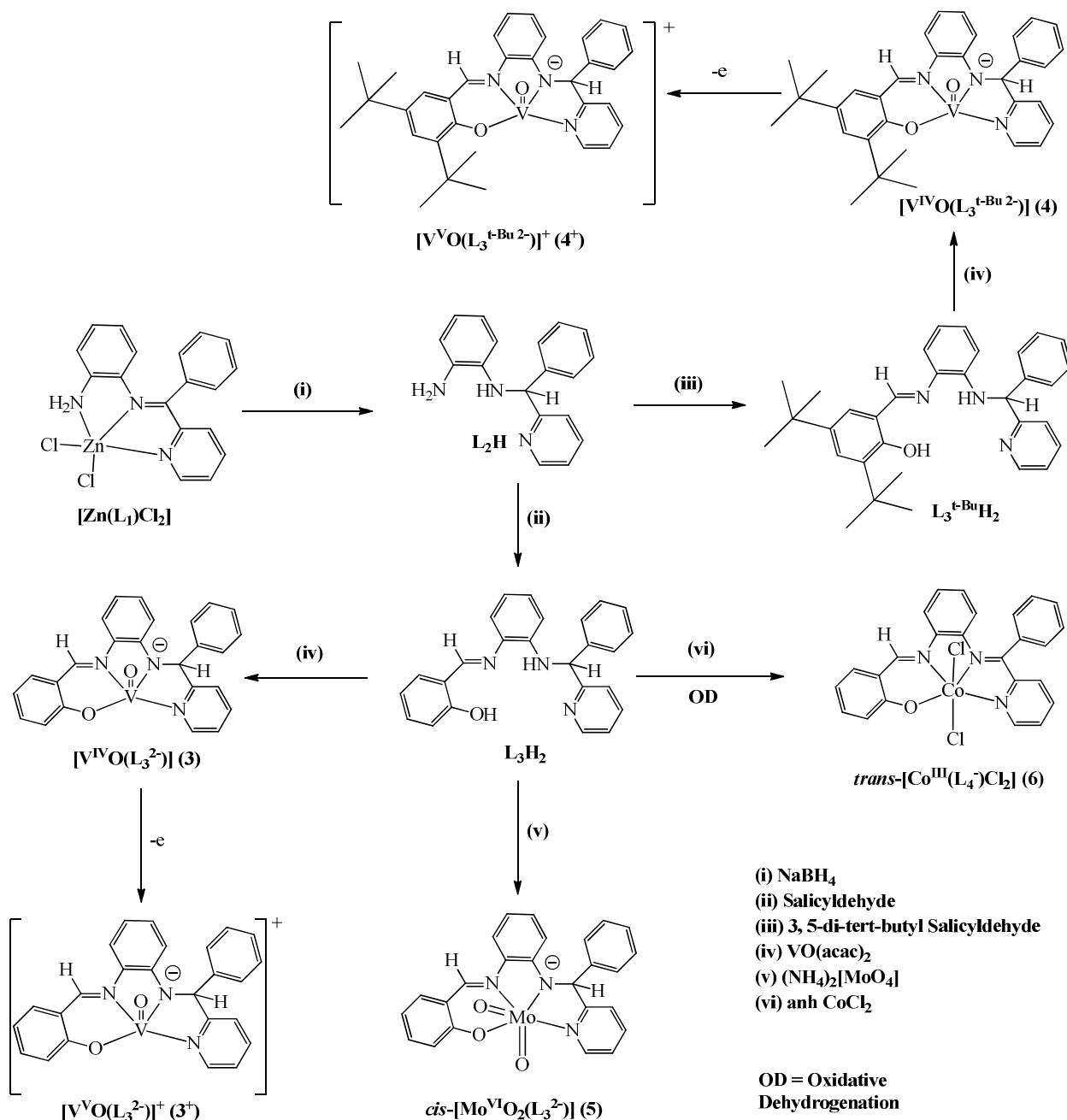
stretching vibrations of **3** and **4** are 966 and 959 cm^{-1} while the symmetric and asymmetric stretching vibrations of two cis $\text{Mo}=\text{O}^{25}$ resonate at 901 and 915 cm^{-1} . UV/vis absorption spectral data are summarized in Table 2. UV/vis spectra are shown in Fig. S1. The lower energy absorption bands of **3** and **4** disappear in **3**⁺ and **4**⁺ ions. Complexes **5** and **6** do not display any lower energy absorption bands.

The paramagnetic **3** and **4** complexes are redox active. The redox series of **3** and **4** were investigated by cyclic voltammetry in CH_2Cl_2 containing 0.2 M tetrabutylammoniumhexafluoro

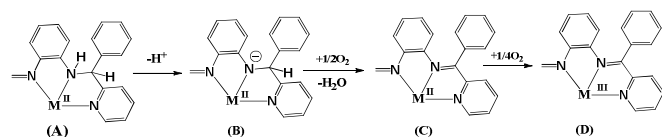
Table 2 UV-vis/NIR absorption spectral data of **3**, **3**⁺, **4**, **4**⁺, **5** and **6** in CH_2Cl_2 at 298 K

Comp	λ_{max} (ϵ , $104 \text{ M}^{-1} \text{ cm}^{-1}$), nm
3	496 (0.28), 386 (0.44), 327 (0.51)sh, 313 (0.80) sh, 300 (1.24), 266 (1.67)
3 ⁺	491 (0.13)sh, 407 (0.33)sh, 376 (0.49), 331 (0.64)sh
4	492 (0.43), 393 (0.63), 333 (1.72)sh, 316 (2.30) sh, 298 (2.78), 264 (3.20)
4 ⁺	512 (0.13)sh, 421 (0.55), 357 (0.74)sh
5	450 (0.31), 351 (1.01), 326 (1.71)sh 310 (2.23), 256 (2.67)sh
6	423 (0.24), 352 (0.41)sh, 331 (0.53)sh, 303 (0.66), 250 (1.10), 206 (1.74)

Scheme 2



Scheme 3



phosphate as supporting electrolyte. Cyclic voltammogram of **3** is shown in Fig. S2. The anodic redox waves of **3** and **4** at 0.35 and 0.33 V are assigned to $\text{VO}^{3+}/\text{VO}^{2+}$ redox couple.

No electron transfer occurs in the reactions of L_3H_2 with $\text{VO}(\text{acac})_2$ and molybdate ion producing amide complexes **3**, **4** and **5**. However, the reaction of CoCl_2 with L_3H_2 affords ketimine complex, **6**. In the reaction with CoCl_2 , both the metal ion and the ligand undergo oxidation. Overall it is a $-(3e+2H^+)$ transfer reaction involving external dioxygen molecule as an oxidizing agent. Scheme 3 illustrates the probable intermediates of this $-(3e+2H^+)$ transfer redox reaction which involves: the coordination of the $\text{M}(\text{II})$ ion to the monoanionic L_3H^- ligand affording **A**, deprotonation of the monoanionic L_3H^- ligand to the dianionic L_3^{2-} affording **B**, the oxidation of the dianionic L_3^{2-} to L_4^- by external oxygen molecule affording **C**. The intermediate **A** has been isolated as a iron (III) complex as **1** (Scheme 1).⁷ The intermediate **B** has been isolated as oxidovanadium(IV) and *cis*-dioxidomolybdenum(VI) complexes as **3**, **4** and **5**. In case of ruthenium, **C** is the final product furnishing 2^+ ion (Scheme 1). However, in case of cobalt(II) ion, the e_g^1 electron is delocalized over the low-lying π_{diimine}^* orbital and reacts easily with air affording cobalt(III) complex, **D**.

The OD reaction with the cobalt(II) ion is informative. The higher valent cobalt(IV) ion will never be achieved in air and cobalt(III) ion even achieved is not an oxidizing agent. It completely defies the participation of higher oxidation state of the metal ion in an OD reaction of the amine. One of the important roles of the metal ions is to de-protonate the NH function upon coordination, which is achieved in cases of oxidovanadium and oxidomolybdenum ions. The oxidation occurs by the external O_2 molecule to facilitate the $d_M \rightarrow \pi_{\text{imine}}^*$ back-bonding which is favored with a t_2^6 state, e.g. Ru(II) and Co(III) ions. For effective back-bonding increasing the M-N bond order, it needs lower oxidation state of the metal ions. Oxidovanadium(IV) and dioxidomolybdenum(VI) ions in **3-5** are respectively d^1 and d^0 ions and lacks the ability to back donate significantly disfavoring the OD of the amide ligand.

Molecular geometries

Molecular bond parameters and cis or trans geometries of **3-6** were confirmed by the single crystal X-ray structure determinations of $4\cdot\text{CH}_3\text{OH}$, **5** and **6**. $4\cdot\text{CH}_3\text{OH}$ crystallizes in *P*-1 space group. The molecular geometry of $4\cdot\text{CH}_3\text{OH}$ in the crystals with the atom labeling scheme is illustrated in Fig. 1. Significant bond parameters are summarized in Table 3. The tetra-dentate $\text{L}_3^{\text{t-Bu}}^{2-}$ dianionic ligand spans the sites of the square (with a mean deviation of 0.09 Å) of the distorted square pyramid coordination sphere around the vanadium ion. The

vanadium ion is displaced towards the oxido group by 0.65 Å. The oxidovanadium, V(1)-O(40) and the V(1)-O_{phenolato} *i.e.* V(1)-O(1) bond lengths, respectively 1.612(2) and 1.925(2) Å, correlate well with the presence of the oxidovanadium(IV) ion in $4\cdot\text{CH}_3\text{OH}$.²⁶ The C(8)-N(9) and C(17)-N(16) lengths, 1.303(3) and 1.448(3) Å, are consistent with the existence of the aldimine, $-\text{CH}=\text{N}-$ and $(\text{Ph})(\text{Py})(\text{H})\text{C}-\text{N}(\text{H})-$ functions in $4\cdot\text{CH}_3\text{OH}$.⁷

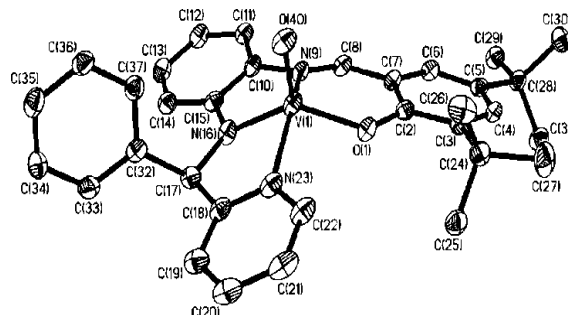


Fig. 1 Molecular geometry of $4\cdot\text{CH}_3\text{OH}$ in crystals (50% ellipsoids; CH_3OH and H atoms are omitted for clarity).

Table 3 Selected experimental bond lengths (Å) and angles (°) of $4\cdot\text{CH}_3\text{OH}$ and corresponding calculated parameters of **3**

	Exp	Cal
	$4\cdot\text{CH}_3\text{OH}$	3
V(1)-O(1)	1.925(2)	1.923
V(1)-N(9)	2.052(2)	2.066
V(1)-N(16)	1.950(2)	1.968
V(1)-N(23)	2.099(3)	2.110
V(1)-O(40)	1.612(2)	1.599
C(8)-N(9)	1.303(3)	1.302
N(16)-C(17)	1.448(3)	1.448
O(1)-V(1)-N(16)	135.08(9)	133.75
N(9)-V(1)-N(23)	146.09(10)	147.79

5 crystallizes in *P*-1 space group. An ORTEP plot of the molecule and the atom labeling scheme are illustrated in Fig. 2. Significant bond parameters are listed in Table 4. The orientation of the L_3^{2-} ligand in **5** is different from that in $4\cdot\text{CH}_3\text{OH}$. The Mo-N_{py} (N(23)) bond is perpendicular to the MoO(1)N(9)N(16) plane making two oxido groups cis to each other. Two Mo=O bond lengths, 1.7096(11) and 1.7198(11) Å,

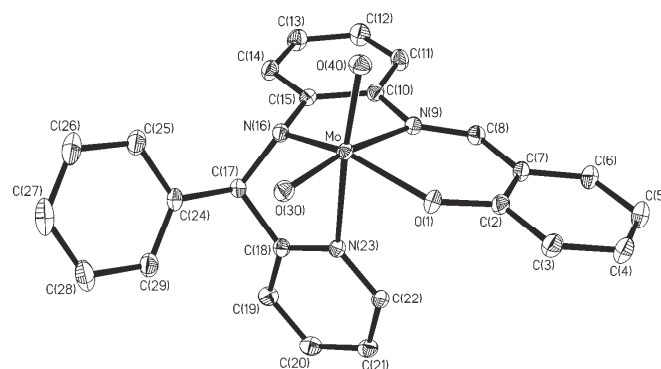


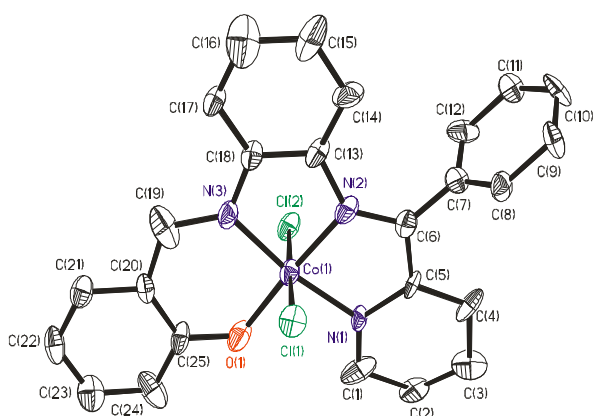
Fig. 2 Molecular geometry of **5** in crystals (50% ellipsoids; H atoms are omitted for clarity).

Table 4 Selected experimental bond lengths (Å) and angles (°) of **5**

Mo-O(1)	1.9692(11)	C(8)-N(9)	1.2934(19)
Mo-N(9)	2.2958(13)	N(16)-C(17)	1.4789(18)
Mo-N(16)	2.0219(12)	O(1)-Mo-N(16)	147.57(5)
Mo-N(23)	2.3637(12)	N(9)-Mo-N(23)	77.79(4)
Mo-O(30)	1.7198(11)	O(40)-Mo-O(30)	107.32(5)
Mo-O(40)	1.7096(11)		

are similar to those reported in *cis*-dioxidomolybdenum(VI) complexes.²⁵ The C(8)-N(9) length, 1.294(2) Å, authenticates the aldimine (-CH=N-) function while C(17)-N(16) length, 1.479(2) correlates well with a C-N single bond.

6 crystallizes in $P2_1/c$ space group. The molecular geometry of **6** in the crystals with the atom labeling scheme is depicted in Fig. 3. Significant bond parameters are summarized in Table 5. The orientation of the tetra-dentate L_4^- ligand is different from the dianionic $L_3^{t-Bu 2-}$ and L_3^{2-} ligands present in **4**, **CH₃OH** and **5**. In contrast to the non-planar geometries of $L_3^{t-Bu 2-}$ and L_3^{2-} , the L_4^- in **6** is completely planar excluding the pendent phenyl group and occupies a square plane of the CoN_3OCl_2 octahedron enforcing the two chloride ligands trans to each other.

**Fig. 3** Molecular geometry of **6** in crystals (50% ellipsoids; H atoms are omitted for clarity).**Table 5** Selected experimental and calculated bond lengths (Å) and angles (°) of **6**

	Exp	Cal
Co(1)-O(1)	1.872(2)	1.888
Co(1)-N(1)	1.933(3)	1.9451
Co(1)-N(2)	1.880(3)	1.916
Co(1)-N(3)	1.870(3)	1.896
Co(1)-Cl(1)	2.2333(10)	2.306
Co(1)-Cl(2)	2.2637(10)	2.306
N(2)-C(6)	1.285(4)	1.299
N(3)-C(19)	1.297(4)	1.306
Cl(1)-Co(1)-Cl(2)	177.55(4)	177.33
O(1)-Co(1)-N(2)	176.30(12)	176.85
N(3)-Co(1)-N(1)	170.08(13)	169.75

The N(3)-C(19) and N(2)-C(6) lengths, 1.285(4) and 1.297(4) Å, are consistent with the existence of the aldimine (-CH=N-) and ketimine ((Ph)(py)C=N-) functions in **6**.⁷ The bond parameters and the planarity confirm the $-(2e+2H^+)$ oxidation

of L_3^{2-} to L_4^- in **6**. Two trans Co^{III} -Cl lengths are 2.233(2) and 2.364(2) Å.

Table 6 Significant experimental M-N_{imine}, M-N_{amide} and M-N_{ketimine} bond lengths (Å)

Bond Type	Length	Complexes
Fe ^{III} -N _{amine}	2.192(2)	1
Ru ^{II} -N _{ketimine}	1.976(6)	2⁺
V ^{IV} -N _{amide}	1.950(2)	4
Mo ^{VI} -N _{amide}	2.022(2)	5
Co ^{III} -N _{ketimine}	1.880(3)	6

The trend of M-N_{ketimine} and M-N_{amine} bond lengths in **1-6** complexes is noteworthy. All the three types of bond lengths, M-N_{amine}, M-N_{amide} and M-N_{ketimine} with 3d and 4d metal ions have successfully been determined. The experimental bond lengths are listed in Table 6. It is observed that the M-N_{ketimine} lengths are significantly shorter than the M-N_{amine} and M-N_{amide} lengths. In **2⁺**, the Ru^{II}-N_{ketimine} length, 1.976(6) Å, is intermediate between the reported Ru^{II}-N_{amine} and Ru^{II}=N_{imide} lengths. The average Ru^{II}-N_{amine} and Ru^{II}-N_{iminoquinone} distances in *o*-phenylenediamine complexes are 2.132 and 2.080 Å.²⁷ The reported average Ru^{II}=N_{imide} length is 1.753 Å.²⁸ It claims that the bond order of the Ru^{II}-N_{ketimine} in **2⁺** ion is higher than one. Similar trend has been recorded in case of Co(III) complex, **6** also. The Co^{III}-N_{imine} distance, 1.880(3) Å, is shorter than Fe^{III}-N_{amine} and V^{IV}-N_{amide} distances (Table 6). The observed Co^{III}-N_{aldimine} length in **6** is 1.870(3) Å. In a *o*-phenylenediamine complex, Co^{III}-N_{amine} length is 1.982(8)-2.016(3) Å,²⁹ while the Co^{III}=N_{imide} length in a cobalt(III) aryl imido complex is 1.675 Å.³⁰ In **6**, the Co^{III}-N_{ketimine} length being intermediate of the Co^{III}-N single and double bonds corresponds to a bond order higher than one. The features are explained by the mixing of the $d_M-\pi^*$ orbitals (*vide infra*) that stabilizes the lower oxidation states of the metal ions and increases the M-N_{ketimine} bond order.

EPR spectra, fluorescence and fluorescence-spectro electro chemistry

The EPR spectra with simulation are shown in the panels (a-c) of Fig. S3. The spectra with the hyperfine coupling from ⁵¹V nuclei corroborate with $s = 1/2$ spin state and (**3**, $g_{iso} = 1.9806$, $A = 86.9 \times 10^{-4} \text{ cm}^{-1}$; **4**, $g_{iso} = 1.9778$, $A = 86.7 \times 10^{-4} \text{ cm}^{-1}$) and are consistent with the presence of the oxidovanadium(IV) ion in **3** and **4**. The g values of the axial spectrum (panel (b) of Fig. S3) of the CH_2Cl_2 frozen glass of **3** at 25 K are: $g_{||} = 1.9590$, $A_{||} = 156.4 \times 10^{-4} \text{ cm}^{-1}$; $g_{\perp} = 1.9828$, $A_{\perp} = 103.7 \times 10^{-4} \text{ cm}^{-1}$. Analyses of the EPR spectra of **3⁺** and **4⁺** ions confirm that the oxidation is metal centered concluding **3⁺** and **4⁺** cations are the oxidovanadium(V) complexes of types $[V^VO(L_3^{2-})]^+$ (**3⁺**) and $[V^VO(L_3^{t-Bu 2-})]^+$ (**4⁺**).

3 and **4** are non emissive while the oxidized analogues **3⁺** and **4⁺** ions are emissive at 298 K. In CH_2Cl_2 , **5** and **6** are also fluorescent. The fluorescence data are listed in Table 7 and the relevant spectra are shown in Fig. S4.

Table 7 Fluorescence spectral parameters of the complexes in CH₂Cl₂ at 298 K

Comp	$\lambda_{\text{ex}} / \lambda_{\text{em}} \text{ (nm)} / \phi$
3 ⁺	331/444
4 ⁺	339/490
5	336/466/0.003
6	324/473/0.027

$\phi = \text{Quantum yield}$

In this regard, it is to be noted that the free L₃H₂ ligand is fluorescent ($\lambda_{\text{ex}} = 330$; $\lambda_{\text{em}} = 470$ nm) due to the internal charge transfer from the $\pi_{\text{phenolato}} \rightarrow \pi_{\text{aldimine}}^*$ orbital.⁷ **3** and **4** absorb strongly at comparatively longer wave lengths (493 and 497 nm) due to $\pi_{\text{NPh}} \rightarrow \pi_{\text{aldimine}}^*$ transition and the complexes are non emissive. However similar to **1**, in **3**⁺ and **4**⁺ ions these lower energy bands are absent and the cations are fluorescent.

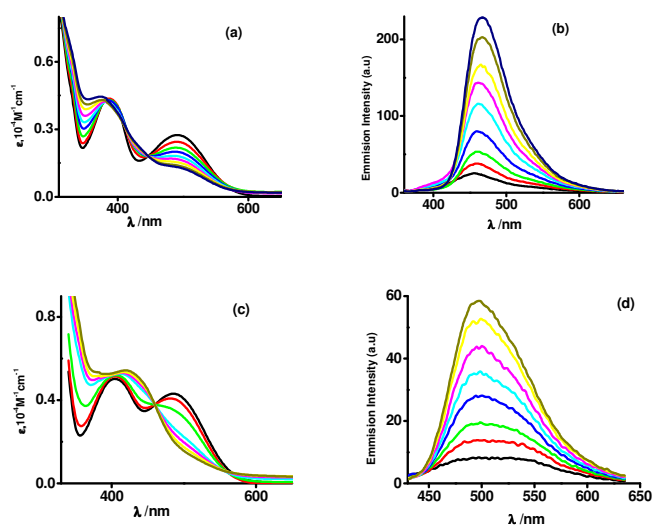


Fig. 4 Spectroelectrochemical measurements of the conversion of **3** \rightarrow **3**⁺ [(a) UV-vis/NIR absorption and (b) fluorescence spectra] and **4** \rightarrow **4**⁺ [(c) UV-vis/NIR absorption and (d) fluorescence spectra] in CH₂Cl₂ at 298 K.

It is to be noted that upon oxidation the lower energy absorption bands gradually disappear while fluorescence intensity at $\lambda_{\text{em}} = 444$ and 490 nm respectively for **3**⁺ and **4**⁺ cations gradually increases as depicted in the panel (b) of Fig. 4. The spectral features of **3**⁺ and **4**⁺ cations are illustrated in Fig. 4. The lower energy absorption bands of **5** and **6** at 450 and 423 nm are weaker and both the complexes are weakly fluorescent as illustrated in Fig. S4 and Table 7.

The origins of the UV-vis/NIR absorptions of **3-6** were elucidated by the time dependent (TD) density functional theory (DFT) calculations on **3**, **3**⁺ and **6**. Gas phase geometry of **3** was optimized at the B3LYP/DFT level with the doublet spin state while those of **3**⁺ and **6** were optimized with the singlet spin state. Calculated bond parameters are listed in Tables 3, 5 and S1. The calculated bond parameters are similar to those obtained from the single crystal X-ray diffraction studies of **4**.CH₃OH and **6** (Tables 3 and 5). The optimized geometries of **3**, **3**⁺ and **6** are shown in Fig. S2. Excitation

energies were calculated by the TD DFT calculations on the optimized geometries. The excitation energies with the oscillator strengths are listed in Table S2. Fragmentations of the ligand used for the calculations are shown in Fig. S5. It is reported that L₃H₂ is emissive due to $\pi_{\text{Phenolato}} \rightarrow \pi_{\text{aldimine}}^*$ transition at $\lambda_{\text{ex}} = 330$ nm. **3** and **4** with lower energy absorption bands at $\lambda_{\text{max}} = 490$ and 500 nm are non-emissive. The TD DFT calculation on **3** has authenticated that the lower energy absorption band of **3** at $\lambda_{\text{max}} = 493.57$ nm with $f = 0.13$ is due to $\pi_{\text{NPh}} \rightarrow \pi_{\text{aldimine}}^*$ transitions. The $\pi_{\text{phenolato}} \rightarrow \pi_{\text{aldimine}}^*$ transition of **3** appears at 316.72 nm. However, the non-emissive lower energy absorption band at $\lambda_{\text{max}} = 490$ nm gradually disappears upon oxidation of **3** to **3**⁺ (panel (a) of Fig. 4) and **3**⁺ becomes emissive. The calculated excitation band of **3**⁺ at 357.8 nm with $f = 0.12$ is due to $\pi_{\text{phenolato}} \rightarrow \pi_{\text{aldimine}}^*$ transition. Similarly, the calculated $\pi_{\text{phenolato}} \rightarrow \pi_{\text{aldimine}}^*$ emissive excitation wave length of **6** is 318.06 nm ($f = 0.45$). The emissive and non-emissive transitions of **3-6** including the L₃H₂ ligand are illustrated in Scheme S1.

Molecular orbital analyses

The constituents of the frontier molecular orbitals of **3** and **6** were investigated by the density functional theory (DFT) calculations using B3LYP functional. Gas phase geometries of **3** and **6** were optimized respectively with doublet and singlet spin states. The constituents of the frontier orbitals are analyzed and the data are summarized in Table S3. The calculations authenticated a significant mixing among the d orbitals and the benzoyl pyridine fragment of the L₄⁻ ligand in **6**. Analyses have shown that the d_{xz} (HOMO-12) and d_{yz} (HOMO-11) orbitals of the t₂ set of **6** exhibit strong interactions with the benzoyl pyridine fragment of the tetra dentate diimine ligand. Similar types of mixing among the d orbitals and the L₄⁻ ligand have been attributed in case of **3** also. However, the d orbitals of the t₂ set of the OV(IV) ion interact equally with the phenolato and the benzoyl pyridine fragments. The mixing of the d orbitals results in diverse effects in **3** and **6**. In case of **6**, the d⁶ ion promotes the oxidation of amine to ketimine for π delocalization while the d¹ ion stabilizes the hard amide binding in **3**. Similarly, the amide binding is stabilized by the hard acid, d⁰, molybdenum(VI) ion. The result is reverse with the soft d⁶ ruthenium(II) ion that converts amine to ketimine for π -delocalization. The OD of the amine to ketimine parallels the chemistry of the conversion of NO \rightarrow NO⁺ reducing metal ions in some cases for effective back-bonding with the lower oxidation states of the metal ions. The results correlate well with the reported conversions of copper(II) to copper(I), d¹⁰ ion, iron(III) to iron(II) t₂⁶ ion and ruthenium(III) to ruthenium(II), t₂⁶ ion oxidizing amines to imines.⁴

Conclusion

The role of the oxidation states of the metal ions in oxidative dehydrogenation (OD) reaction of the (Ph)(Py)(H)C-N(H)-function of an *o*-phenylenediamine derivative (L₃H₂) has been investigated (L₃H₂ = (*E*)-2-(((2-((phenyl(pyridin-2-yl)methyl)

amino)phenyl)imino)methyl)phenol)). Recently, we reported that the reaction of L_3H_2 with anhydrous $FeCl_3$ affords the amine complex *cis*- $[Fe^{III}(L_3H)Cl_2]$ (**1**) while the same reaction with $[Ru^{II}(PPh_3)_3Cl_2]$ results in a OD reaction affording a ketimine complex, *trans*- $[Ru^{II}(L_4)(PPh_3)]^+$ (**2⁺**) in good yields ($L_4H = 2-((E)-(2-((E)-phenyl(pyridin-2-yl)methyleneamino)phenylimino)methyl)phenol)$). To summarize the effect of the higher oxidation states of the metal ions to the OD reaction of L_3H_2 , similar reactions of L_3H_2 with oxidovanadium(IV) and oxidomolybdenum(VI) ions were performed. In each case the reaction produces amide complexes of type $[V^{IV}O(L_3^{2-})]$ (**3**), $[V^{IV}O(L_3^{t-Bu\ 2-})]$ (**4**) and *cis*- $[Mo^{VI}O_2(L_3^{2-})]$ (**5**). However, the reaction of anhydrous $CoCl_2$ with L_3H_2 promotes the OD reaction in air yielding a ketimine complex of type, *trans*- $[Co^{III}(L_4)Cl_2]$ (**6**). The study infers that the OD reaction of L_3H_2 is not successful with the hard metal ions with higher oxidation states, like Fe^{III} , $V^{IV}O$ and $Mo^{VI}O_4$ ions, while the OD reaction occurs with softer, lower valent Ru(II) and Co(II) ions with the filled t_2^6 set that enhances the $d_M \rightarrow p_\pi^*$ back bonding. The work does not justify the previous reports those claim that the metal ion promoted OD reaction of an amine requires the higher oxidation state as an intermediate for oxidation of amines. The work rather concludes that the coordinated amine is de-protonated to amide that undergoes oxidation to ketimine by external oxygen molecule to have stronger $d_M \rightarrow p_\pi^*$ back bonding with the lower oxidation states of the metal ions.

Fluorescence features of L_3H_2 and **3-6** are noteworthy. L_3H_2 is weakly fluorescent ($\lambda_{ex} = 330$; $\lambda_{em} = 470$ nm) due to a non-emissive lower energy absorption band at 390 nm. **3** and **4** exhibit absorption bands at 493 and 497 nm and are non-emissive, while upon oxidation the lower energy absorption band disappears and $[V^{IV}O(L_3^{2-})]^+$ (**3⁺**) and $[V^{IV}O(L_3^{t-Bu\ 2-})]^+$ (**4⁺**) cations are fluorescent recorded by fluorescence-spectro electrochemical measurements in CH_2Cl_2 at 298 K. **5** and **6** display weaker absorption bands at 445 and 423 nm and are weakly fluorescent (**5**, $\lambda_{ex} = 336$ nm, $\lambda_{em} = 466$ nm; **6**, $\lambda_{ex} = 324$ nm, $\lambda_{em} = 473$ nm). Moreover, in addition to the oxidation state dependent fluorescence features of **3-4**, and oxidovanadium(IV) and dioxidomolybdenum(VI) compounds being effective catalysts for several organic transformations, complexes **3-5** appeared to be significant in the coordination chemistry.

Acknowledgements

Financial support received from DST (SR/S1/IC/0026/2012) and CSIR (01/2699/12-EMR-II) New Delhi, India is gratefully acknowledged. SB (CSIR no. 8/531(0006)/2012-EMR-I) and MKB (CSIR no. 8/531(0007)/2012-EMR-I) are thankful to CSIR, New Delhi, India, for fellowships.

Notes and references

^aDepartment of Chemistry, R. K. Mission Residential College, Narendrapur, Kolkata-700103, India. E-mail: ghosh@pghosh.in; Fax: +91 33 2477 3597; Tel: +91 33 2428 7347

^bMax-Planck Institute for Chemical Energy Conversion, Stifstr. 34-36, 45470, Mülheim an der Ruhr, Germany.

[†]Electronic Supplementary Information (ESI) available: UV-vis/NIR absorption spectra (Fig. S1), cyclic voltammogram of **3** (Fig. S2), X-band EPR spectra of **3** and **4** (Fig. S3), fluorescence spectra of **5** and **6** (Fig. S4), photoactive molecular orbitals (Scheme S1), schematic diagram of the ligand fragmentation considered in MO analyses (Fig. S5), Calculated bond lengths of **3**, **3⁺** and **6** (Table S1), TD DFT calculations (Table S2), population analyses of selected molecular orbitals of **6**, **3**, **3⁺** (Table S3) and optimized coordinates (Table S4-S6). For ESI and crystallographic data in CIF or other electronic format see DOI: 10.1039/b000000x/

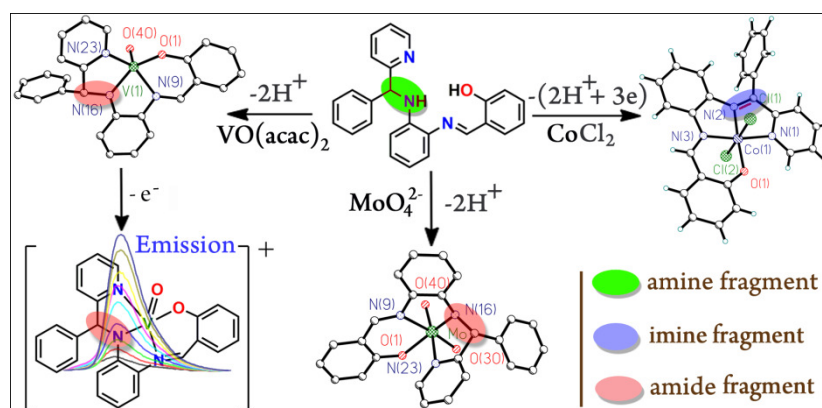
- (a) C. Anthony, *Biochem. J.*, 1996, **320**, 697; (b) P. F. Knowles, D. M. Dooley, H. Sigel and A. Sigel, (Eds.), *Metal Ions in Biological Systems*. Marcel Dekker, New York, 1994, **30**, 361; (c) M. D. Berry, A. V. Juorio and I. A. Paterson, *Prog. Neurobiol.*, 1994, **42**, 375; (d) W. S. McIntire, C. Hartmann and V. L. Davison, (Eds.), *Principles and Applications of Quinoproteins*, Marcel Dekker, New York, 1993, 97; (e) H. Blaschko, *Rev. Physiol Biochem Pharmacol.*, 1974, **70**.
- (a) N. F. Curtis, *J. Chem. Soc. A*, 1971, 2834; (b) N. F. Curtis, *Coord. Chem. Rev.*, 1968, **3**, 3; (c) N. F. Curtis, Y. M. Curtis and H. K. J. Powell, *J. Chem. Soc. A*, 1966, 1015.
- (a) F. R. Keene, *Coord. Chem. Rev.*, 1999, **187**, 121; (b) S. Minakata, Y. Ohshima, A. Takemiya, I. Ryu, M. Komatsu and Y. Ohshiro, *Chemistry Letters*, 1997, **26**, 311; (c) A. J. Bailey and B. R. James, *Chem. Commun.*, 1996, 2343; (d) P. Muller and D. M. Gilbert, *Tetrahedron*, 1988, **44**, 7171; (e) S. I. Murahashi, T. Naota and H. Taki, *J. Chem. Soc. Chem. Commun.*, 1985, 613; (f) C. K. Poon and C. -M. Che, *J. Chem. Soc., Dalton Trans.*, 1981, 1019.
- (a) M. J. Ridd and F. R. Keene, *J. Am. Chem. Soc.*, 1981, **103**, 5733; (b) F. R. Keene, M. J. Ridd and M. R. Snow, *J. Am. Chem. Soc.*, 1983, **105**, 7075; (c) P. Bernhard, D. J. Bull, H.-B. Burgi, P. Gsvath, A. Raselli and A. M. Sargeson, *Inorg. Chem.*, 1997, **36**, 2804; (c) (i) P. Bernhard, D. J. Bull, H. -B. Burgi, P. Gsvath, A. Raselli and A. M. Sargeson, *Inorg. Chem.*, 1997, **36**, 2804; (ii) P. Bernhard and A. M. Sargeson, *J. Chem. Soc. Chem. Commun.*, 1985, 1516; (iii) P. Bernhard, A. M. Sargeson and F. C. Anson, *Inorg. Chem.*, 1988, **27**, 2754; (iv) P. Bernhard and A. M. Sargeson, *J. Am. Chem. Soc.*, 1989, **111**, 597; (v) P. Bernhard and F. C. Anson, *Inorg. Chem.*, 1989, **28**, 3272; (d) M. J. Ridd, D. J. Gakowski, G. E. Sneddon and F. R. Keene, *J. Chem. Soc., Dalton Trans.*, 1992, 1949; (e) F. R. Keene, P. A. Lay, G. E. Sneddon and G.W. Whebell, *Aust. J. Chem.*, 1993, **46**, 1763; (f) (i) P. A. Lay, A. M. Sargeson, B. W. Skelton and A. H. White, *J. Am. Chem. Soc.*, 1982, **104**, 6161; (ii) P. A. Lay and A. M. Sargeson, *Inorg. Chim. Acta.*, 1992, **449**, 198; (g) P. Maruthamuthu, L. K. Patterson and G. Ferraudi, *Inorg. Chem.*, 1978, **17**, 3157.
- (a) (i) G. J. Christian, A. Llobet and F. Maseras, *Inorg. Chem.*, 2010, **49**, 5977; (ii) G. J. Christian, A. Arbuse, X. Fontrodona, M. A. Martinez, A. Llobet and F. Maseras, *Dalton Trans.*, 2009, 6013; (b) D. Wang, Y. Shiraishi and T. Hirai, *Chem. Commun.*, 2011, **47**, 2673; (c) V. Amendola, L. Fabbrizzi, E. Mundum and P. Pallavicini, *Dalton Trans.*, 2003, 773; (d) J. P. Saucedo-Va'zquez, V. M. Ugalde-Saldi'var, A. R. Toscano, P. M. H. Kroneck and M. E. Sosa-Torres, *Inorg. Chem.*, 2009, **48**, 1214; (e) Y. kuroda, N. Tanaka, M. Goto and T. Sakai, *Inorg. Chem.*, 1978, **17**, 314; (f) R. Mitsuhashi, T. Suzuki and Y. Sunatsuki, *Inorg. Chem.*, 2013, **52**, 10183; (g) (i) C. L. Weeks, P. Turner, R. R. Fenton and P. A. Lay, *J. Chem. Soc., Dalton*

- Trans.*, 2002, 931. (ii) R. K. Wilson and S. Brooker, *Dalton Trans.*, 2013, **42**, 12075; (h) A. Panja and P. Guionneau, *Dalton Trans.*, 2013, **42**, 5068; (i) Q. Li, S. Zhou, S. Wang, X. Zhu, L. Zhang, Z. Feng, L. Guo, F. Wang and Y. Wei, *Dalton Trans.*, 2013, **42**, 2861.
6. (a) N. L. Fry, M. J. Rose, D. L. Rogow, C. Nyitray, M. Kaur and P. K. Mascharak, *Inorg. Chem.*, 2010, **49**, 1487; (b) M. J. Rose and P. K. Mascharak, *Inorg. Chem.*, 2009, **48**, 6904; (c) M. J. Rose, N. M. Betterley and P. K. Mascharak, *J. Am. Chem. Soc.*, 2009, **131**, 8340; (d) G. M. Halpenny and P. K. Mascharak, *Inorg. Chem.*, 2009, **48**, 1490; (e) M. J. Rose, C. Nyitray and P. K. Mascharak, *Inorg. Chem.*, 2008, **47**, 11604; (f) M. J. Rose, N. L. Fry, R. Marlow, L. Hinck and P. K. Mascharak, *J. Am. Chem. Soc.*, 2008, **130**, 8834.
7. S. Chaudhuri, S. C. Patra, P. Saha, A. S. Roy, S. Maity, S. Bera, P. S. Sardar, S. Ghosh, T. Weyhermueller and P. Ghosh, *Dalton Trans.*, 2013, **42**, 15028.
8. Vanadium references: (a) M. Li, W. Ding, B. Baruah, D. C. Crans and R. J. Wang, *Inorg. Biochem.*, 2008, **102**, 1846; (b) D. Rehder, *Bioinorganic Vanadium Chemistry*; John Wiley & Sons, Ltd.: New York, 2008; (c) C. J. Schneider and V. L. Pecoraro, *Vanadium: The Versatile Metal*; ACS Symposium Series 974; American Chemical Society: Washington, DC, 2007, 148; (d) D. C. Crans, J. J. Smee, E. Gaidamauskas and L. Yang, *Chem. Rev.*, 2004, **104**, 849.
9. Molybdenum references: (a) R. Hille, *Dalton Trans.*, 2013, **42**, 3029 and the references is there in; (b) Y. Zhang, S. Rump and V. N. Gladyshev, *Coord. Chem. Rev.*, 2011, **255**, 1206; (c) R. Hille, *Chem. Rev.*, 1996, **96**, 2757.
10. (a) (i) R. Dinda, P. Sengupta, S. Ghosh, H. Mayer-Figge and W. S. Sheldrick, *J. Chem. Soc. Dalton Trans.*, 2002, 4434; (ii) C. J. Whiteoak, G. J. P. Britovsek, V. C. Gibson and A. J. P. White, *Dalton Trans.*, 2009, 2337; (b) (i) M. A. Katkar, S. N. Rao and H. D. Juneja, *RSC Adv.*, 2012, **2**, 8071; (ii) Z. Li, S. Wu, H. Ding, H. Lu, J. Liu, Q. Huo, J. Guan and Q. Kan, *New J. Chem.*, 2013, **37**, 4220; (c) P. M. Reis, C. C. Romão and B. Royo, *Dalton Trans.*, 2006, 1842; (d) M. R. Maurya, U. Kumar and P. Manikandan, *Dalton Trans.*, 2006, 3561; (e) R. A. Row and M. M. Jones, *Inorg. Synth.*, 1957, **5**, 113.
11. (a) H. Xiang, J. Cheng, X. Ma, X. Zhou and J. Chruma, *J. Chem. Soc. Rev.*, 2013, **42**, 6128; (b) M. D. Ward, *Coord. Chem. Rev.*, 2010, **254**, 2634; (c) V. W. W. Yam, (Ed.) *Photofunctional Transition Metal Complexes*; Springer: Series: Structure and Bonding, 2007, Vol. 123; (d) M. D. Ward, *Coord. Chem. Rev.*, 2007, **251**, 1663; (e) M. Hissler, J. E. McGarrah, W. B. Connick, D. K. Geiger, S. D. Cummings and R. Eisenberg, *Coord. Chem. Rev.*, 2000, **208**, 115.
12. J. R. Lakowicz, *Principles of Fluorescence Spectroscopy*; Springer: Third Edition, 2006.
13. (a) G. M. Sheldrick, *SHELXS97*; Universität Göttingen: Göttingen, Germany, 1997; (b) G. M. Sheldrick, *SHELXL97*; Universität Göttingen: Göttingen, Germany, 1997.
14. M. J. Frisch, Trucks, G. W. H. B. Schlegel, G. E. Scuseria, M. A. Robb, J. R. Cheeseman, Jr. J. A. Montgomery, T. Vreven, K. N. Kudin, J. C. Burant, J. M. Millam, S. S. Iyengar, J. Tomasi, V. Barone, B. Mennucci, M. Cossi, G. Scalmani, N. Rega, G. A. Petersson, H. Nakatsuji, M. Hada, M. Ehara, K. Toyota, R. Fukuda, J. Hasegawa, M. Ishida, T. Nakajima, Y. Honda, O. Kitao, H. Nakai, M. Klene, X. Li, J. E. Knox, H. P. Hratchian, J. B. Cross, V. Bakken, C. Adamo, J. Jaramillo, R. Gomperts, R. E. Stratmann, O. Yazyev, A. J. Austin, R. Cammi, C. Pomelli, J. W. Ochterski, P. Y. Ayala, K. Morokuma, G. A. Voth, P. Salvador, J. J. Dannenberg, V. G. Zakrzewski, S. Dapprich, A. D. Daniels, M. C. Strain, O. Farkas, D. K. Malick, A. D. Rabuck, K. Raghavachari, J. B. Foresman, J. V. Ortiz, Q. Cui, A. G. Baboul, S. Clifford, J. Cioslowski, B. B. Stefanov, G. Liu, A. Liashenko, P. Piskorz, I. Komaromi, R. L. Martin, D. J. Fox, T. Keith, M. A. Al-Laham, C. Y. Peng, A. Nanayakkara, M. Challacombe, P. M. W. Gill, B. Johnson, W. Chen, M. W. Wong, C. Gonzalez and J. A. Pople, *Gaussian 03, revision E.01*; Gaussian, Inc.: Wallingford, CT, 2004.
15. (a) *The Challenge of d and f Electrons*, D. R. Salahub and M. C. Zerner, Eds.; ACS: D.C. Washington, 1989; (b) R. G. Parr and W. Yang, *Density Functional Theory of Atoms and Molecules*; Oxford University Press: Oxford, U.K., 1989; (c) W. Kohn and L. J. Sham, *Phys. Rev.*, 1965, **140**, A1133; (d) P. Hohenberg and W. Kohn, *Phys. Rev.*, 1964, **136**, B864.
16. (a) R. E. Stratmann, G. E. Scuseria and M. Frisch, *J. Chem. Phys.*, 1998, **109**, 8218; (b) M. E. Casida, C. Jamoroski, K. C. Casida and D. R. Salahub, *J. Chem. Phys.*, 1998, **108**, 4439; (c) R. Bauernschmitt and R. Ahlrichs, *Chem. Phys. Lett.*, 1996, **256**, 454.
17. (a) A. D. Becke, *J. Chem. Phys.*, 1993, **98**, 5648; (b) B. Miehlich, A. Savin, H. Stoll and H. Preuss, *Chem. Phys. Lett.*, 1989, **157**, 200; (c) C. Lee, W. Yang and R. G. Parr, *Phys. Rev. B*, 1988, **37**, 785.
18. P. J. Pulay, *Comp. Chem.*, 1982, **3**, 556.
19. H. B. Schlegel and J. J. McDouall, *Computational Advances in Organic Chemistry*, Eds., C. Ogretir, I. G. Csizmadia, Kluwer Academic: The Netherlands, 1991, 167.
20. (a) P. J. Hay and W. R. Wadt, *J. Chem. Phys.*, 1985, **82**, 270; (b) W. R. Wadt and P. J. Hay, *J. Chem. Phys.*, 1985, **82**, 284; (c) P. J. Hay and W. R. Wadt, *J. Chem. Phys.*, 1985, **82**, 299.
21. (a) T. Clark, J. Chandrasekhar, G. W. Spitznagel and P. V. R. Schleyer, *J. Comp. Chem.*, 1983, **4**, 294; (b) P. C. Hariharan and J. A. Pople, *Theo. Chim. Acta.*, 1973, **28**, 213.
22. (a) V. A. Rassolov, M. A. Ratner, J. A. Pople, P. C. Redfern and L. A. Curtiss, *J. Comp. Chem.*, 2001, **22**, 976. (b) M. M. Francl, W. J. Pietro, W. J. Hehre, J. S. Binkley, D. J. DeFrees, J. A. Pople and M. S. Gordon, *J. Chem. Phys.*, 1982, **77**, 3654. (c) P. C. Hariharan and J. A. Pople, *Mol. Phys.*, 1974, **27**, 209; (d) P. C. Hariharan and J. A. Pople, *Theo. Chim. Acta.*, 1973, **28**, 213; (e) W. J. Hehre, R. Ditchfield and J. A. Pople, *J. Chem. Phys.*, 1972, **56**, 2257.
23. N. M. O'Boyle, A. L. Tenderholt and K. M. Langner, *J. Comp. Chem.*, 2008, **29**, 839.
24. (a) M. Cossi, N. Rega, G. Scalmani and V. Barone, *J. Comput. Chem.*, 2003, **24**, 669; (b) V. Barone and M. Cossi, *J. Phys. Chem. A*, 1998, **102**, 1995.
25. (a) J. A. Schachner, P. Traar, C. Sala, M. Melcher, B. N. Harum, A. F. Sax, M. Volpe, F. Belaj and Z. N. C. Mosch, *Inorg. Chem.*, 2012, **51**, 7642; (b) Y. L. Wong, L. H. Tong, J. R. Dilworth, D. K. P. Ng and H. K. Lee, *Dalton Trans.*, 2010, **39**, 4602; (c) C. Zhang, G. Rheinwald, V. Lozan, B. Wu, P. G. Lassahn, H. Lang and C. Janiak, *Z. Anorg. Allg. Chem.*, 2002, **628**, 1259; (d) A. M. Santos, F. E. Kühn, K. B. Jensen, I. Lucas, C. C. Romão and E. Herdtweck, *J. Chem. Soc. Dalton Trans.*, 2001, 1332.

26. (a) S. Kundu, S. Maity, T. Weyhermuller and P. Ghosh, *Inorg. Chem.*, 2013, **52**, 7417; (b) A. S. Roy, P. Saha, N. D. Adhikary and P. Ghosh, *Inorg. Chem.*, 2011, **50**, 2488 and the references therein.
27. A. Lu´ci, R. Silva, M. O. Santiago, I. C. N. Dio´genes, S. O. Pinheiro, E. E. Castellano, J. Ellena, A. A. Batista, F. B. Do-Nascimento, and I. S. Moreira, *Inorg. Chem. Commun.*, 2005, **8**, 1154.
28. R. A. Eikey and M. M. Abu-Omar, *Coord. Chem. Rev.*, 2003, **243**, 83.
29. (a) V. Stavila, A. Gulea, S. Shova, Y. A. Simonov, P. Petrenko, J. Lipkowski, F. Riblet and L. Helm, *Inorg. Chim. Acta.*, 2004, **357**, 2060; (b) Y. Yanase, H. Yoshimura, S. Kinoshita, T. Yamaguchi and H. Wakita, *Acta Cryst.*, 1990, **C46**, 36; (c) L. P. Battaglia, A. M. Corradi, C. G. Palmieri, M. Nardelli and M. E. V. Tani, *Acta Cryst.*, 1974, **B30**, 1114; (d) A. A. Khandar, B. Shaabani, F. Belaj and A. Bakhtiari, *Polyhedron*, 2006, **25**, 1893.
30. X. Hu and K. Meyer, *J. Am. Chem. Soc.*, 2004, **126**, 16322.

Table of contents entry

Formations of the oxidovanadium(IV) and *cis*-dioxidomolybdenum(VI) complexes of the amide derivative of the (Ph)(Py)(H)C-N(H)- function of an *o*-phenylenediamine derivative that in turn is converted to an imine, (Ph)(Py)C=N-, by cobalt(II) ion, contradict the participation of the higher oxidation states to the oxidative dehydrogenation of amines acclaimed so far.



Oxidovanadium(IV), Oxidomolybdenum(VI) and Cobalt(III) Complexes of *o*-Phenylenediamine Derivatives: Oxidative Dehydrogenation and Photoluminescence

Satyabrata Chaudhuri, Sachinath Bera, Manas Kumar Biswas, Amit Saha Roy, Thomas

Weyhermüller and Prasanta Ghosh

Table of contents entry

Formations of the oxidovanadium(IV) and *cis*-dioxidomolybdenum(VI) complexes of the amide derivative of the (Ph)(Py)(H)C-N(H)- function of an *o*-phenylenediamine derivative that in turn is converted to an imine, (Ph)(Py)C=N-, by cobalt(II) ion, contradict the participation of the higher oxidation states to the oxidative dehydrogenation of amines acclaimed so far.

